from each acetate ion and two from the acac ligand with average B–O distances of 1.450 (4) Å and 1.471 (4) Å, respectively; the difference, 0.021 (6) Å, is barely significant. These four oxygen atoms adopt an almost perfect tetrahedral arrangement about the boron with only a slight expansion (i.e., O(5)–B(1)–O(6) = 112.2(3)°) of the angle subtended by the acac oxygen atoms and a small compression (O(1)–B(1)–O(3) = 103.8 (2)°) of the angle between the acetate ligands. In addition to the four oxygen atoms that are directly bonded to the boron atom, there are two additional oxygen atoms, one from each acetate ion, at 2.741 (4) and 2.750 (4) Å from the boron atom. These distances can clearly be interpreted as nonbonded contact distances. If, in describing the geometry about the boron, we include these oxygen atoms as part of the coordination sphere, the geometry about the boron would be described as that of a bicapped tetrahedron.

The acetate ligands show two distinctly different C–O bond lengths with average distances of 1.198 (4) and 1.334 (4) Å, respectively. These distances are consistent with the predominance of contribution A rather than B to the bonding description of the acetate ligands. The average C–O and central HC–C distances of the acac ligand are 1.296 (4) and 1.362 (4) Å, respectively, and are consistent with the fully delocalized description of the acac ligand.

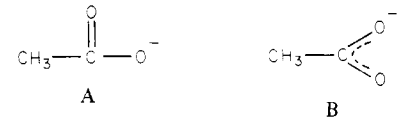

A B

Acknowledgment. We are grateful to the Robert A. Welch Foundation for support under Grant No. A-494.

Registry No. 1, 51455-04-0.

Supplementary Material Available: A listing of observed and calculated structure factors (4 pages). Ordering information is given on any current masthead page.

Contribution from the Departments of Chemistry, Texas A&M University, College Station, Texas 77843, and The Ohio State University, Columbus, Ohio 43210

Survey of the Bonding in Several Structural Types of Trinuclear Molybdenum and Tungsten Cluster Compounds

BRUCE E. BURSTEN,*[1a] F. ALBERT COTTON,*[1b] MICHAEL B. HALL,*[1b] and ROBERT C. NAJJAR[1b]

Received June 8, 1981

The bonding within equilateral triangular clusters of molybdenum and tungsten and the bonding of μ_3-O, μ-O, and μ-Cl to them have been examined by using nonempirical Fenske–Hall calculations. Calculations on the bipyramidal and trigonal-prismatic metal–oxygen "core" species $[Mo_3(\mu_3\text{-}O)_2]^{8+}$ and $[Mo_3(\mu\text{-}O)_6]$ indicate that both capping and edge bridging cause the movement of charge out of the main metal–metal bonding orbitals, resulting in the occupation of higher lying nonbonding and antibonding metal–metal orbitals. The electronic structure of the pyramidal fragment $[Mo_3(\mu_3\text{-}O)(\mu\text{-}O)_3]^{4+}$ is shown to be dominated by the influence of the three edge-bridging μ-O groups. The ability of the trinuclear framework to accommodate a variable number of electrons has been investigated by comparative calculations on $[Mo_3(\mu_3\text{-}O)(\mu\text{-}O)_3]^{4+}$ and $[Mo_3(\mu_3\text{-}O)(\mu\text{-}Cl)_3]^{5+}$, as representatives of the pyramidal type, with six and eight electrons, respectively. The results presented are consistent with the generally longer M–M bonds in systems containing the $M_3(\mu_3\text{-}O)_2$ core relative to those containing the $M_3(\mu_3\text{-}O)(\mu\text{-}O)_3$.

Introduction

Within the past few years a number of studies have shown the discrete equilateral triangle with M–M bonds to be a favored structural element for molybdenum and tungsten in higher oxidation states.[2-8] A comprehensive review with complete references has recently appeared.[9] Since the appearance of that review, several further discoveries that show even more forcefully the importance of such compounds have been reported.[10,11] In this report we shall deal with two structural types, which, apart from some variability in the nature and arrangement of the peripheral ligands, may be classified as follows. In the first type there is a triply bridging, or capping, ligand above the plane of the metal atoms and three edge-briding ligands below it (**1**). In the second type there

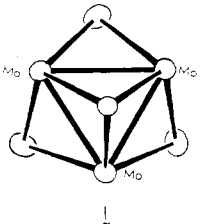

1

are capping ligands on both sides of the metal atom triangle (**2**). We shall refer to these structural types as pyramidal (pyr) and trigonal bipyramidal (tbp), respectively. Both the pyr and the tbp structural types are stable for more than one

(1) (a) The Ohio State University. (b) Texas A&M University.
(2) Bino, A.; Ardon, M.; Maor, I.; Kaftory, M.; Dori, Z. *J. Am. Chem. Soc.* **1976**, *98*, 7093.
(3) Mennemann, K.; Mattes, R. *Angew. Chem.* **1976**, *88*, 92.
(4) Bino, A.; Cotton, F. A.; Dori, Z.; Koch, S.; Küppers, H.; Millar, M.; Sekutowski, J. C. *Inorg. Chem.* **1978**, *17*, 3245.
(5) Bino, A.; Cotton, F. A.; Dori, Z. *J. Am. Chem. Soc.* **1978**, *100*, 5252.
(6) Bino, A.; Cotton, F. A.; Dori, Z. *J. Am. Chem. Soc.* **1979**, *101*, 3842.
(7) Bino, A.; Cotton, F. A.; Dori, Z. *Inorg. Chim. Acta* **1979**, *33*, L133.
(8) Cotton, F. A.; Felthouse, T. R.; Lay, D. G. *J. Am. Chem. Soc.* **1980**, *102*, 1431.
(9) Jostes, R.; Müller, A.; Cotton, F. A. *Angew. Chem., Int. Ed. Engl.* **1980**, *19*, 875.
(10) Bino, A. *J. Am. Chem. Soc.* **1980**, *102*, 7990.
(11) Bino, A.; Cotton, F. A.; Dori, Z. *J. Am. Chem. Soc.* **1981**, *103*, 243.

0020-1669/82/1321-0302$01.25/0

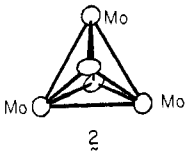

2

mean oxidation state of the metal atoms. Thus, among the characterized pyr structures are the $[Mo_3O_4(C_2O_4)_3(H_2O)_3]^{2+}$ cation[5] and $[Mo_3OCl_3(O_2CCH_3)_3(H_2O)_3]^{2+}$ cation,[7] in which there are formally six and eight electrons, respectively, available for metal–metal bonding. The tbp structures based on molybdenum also show considerably diversity,[11] exhibiting the ability to accommodate both O and CR as capping groups and a variable number of "core" electrons, although the only known tungsten analogues[4] are restricted to those with O atoms as caps and six electrons.

There has been a continuing effort to formulate detailed electronic descriptions of the bonding in equilateral-triangular metal systems.[9,12-16] We have recently reported molecular orbital calculations on Re_3Cl_9, $[Re_3Cl_{12}]^{3-}$, and Re_3Br_9 using both the $X\alpha$–SW and Fenske–Hall molecular orbital formalisms.[15,16] The calculations on the trirhenium(III) cluster compounds not only confirmed the assignment of double bonds between each pair of rhenium atoms but also provided valuable information about the modes of metal–halogen bonding. The bonding in the novel molybdenum and tungsten triangular systems has, thus far, been investigated only by use of the empirical Cotton–Haas (CH) MO method,[12] or a modest extension thereof.[9] Since the CH method, by its very nature, excludes discussion of metal–ligand bonding, we have carried out a more detailed investigation of the electronic structures of these systems, employing the nonempirical Fenske–Hall method.[17] In this paper we report the results of our calculations of the pyr metal ligand cores $[Mo_3O_4]^{4+}$ and $[Mo_3OCl_3]^{5+}$, the *tbp* core $[Mo_3O_2]^{8+}$, and, although no actual example of it has been reported, a trigonal prismatic (tpr) core (**3**) Mo_3O_6, in which there are three edge-bridging oxygen

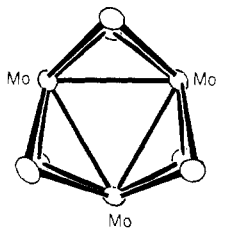

3

atoms on each side of the metal atom triangle. We will also report calculations on $[Mo_3O_4(OH)_6(H_2O)_3]^{2-}$, a model of the oxalato-bridged species cited earlier, in order to assess the effect of peripheral ligands and compare it to a calculation on $[Mo_3O_2(O_2CH)_6(H_2O)_3]^{2+}$, a prototype of a tbp molecule with peripheral ligands.

Calculational Details

The approximate nonempirical molecular orbital method of Fenske and Hall has been described previously.[17] The coordinates for the tbp, pyr, and tpr molybdenum–oxygen cores

Table I. Relative Orbital Energies and Atomic Orbital Population for the Primarily 4d Valence Molecular Orbitals of $[Mo_3]^{12+}$

orbital	rel E, eV	% contribution[b] z^2	x^2-y^2	xy	xz	yz	s	p
$1a_2'$	14.28				83			17
$2e''$	11.30			14		82		4
$3e'$	11.14	89	5		0		2	4
$1a_1''$	10.42			100				
$2e'$	9.45	3	86		8		3	0
$1e''$	5.63			85		15		0
$2a_1'$	5.11	0	98				2	0
$1a_2''$	2.89					99		1
$1e'$[a]	1.88	2	8		84		3	3
$1a_1'$	0	91	0				4	5

[a] Highest occupied orbital. [b] Blank entries are zero by symmetry.

$[Mo_3O_2]^{8+}$, $[Mo_3O_4]^{4+}$, and Mo_3O_6 were idealized to D_{3h} or C_{3v} point symmetry by using bond lengths and angles from the crystal structure of $Cs_2[Mo_3O_4(C_2O_4)_3(H_2O)_3]\cdot 4H_2O\cdot {}^1/_2H_2C_2O_4$.[5] The Mo–Mo distance used was 2.486 Å, and the metal to μ_3-O and μ-O distances were 1.950 and 1.921 Å, respectively. The same metal–metal and metal–oxygen distances were used for $[Mo_3O_4(OH)_6(H_2O)_3]^{2-}$, in which the Mo–OH and Mo–OH_2 distances were assumed to be 2.09 and 2.154 Å, respectively. The results of these calculations were transformed into the canonical orbitals of $[Mo_3]^{12+}$ at the same Mo–Mo distance.

The coordinates for $[Mo_3OCl_3]^{5+}$ were taken from the crystal structure[7] of $[Mo_3OCl_3(O_2CCH_3)_3(H_2O)_3](ClO_4)Cl$ and idealized to C_{3v} symmetry. The Mo–Mo, Mo–O, and Mo–Cl distances used were 2.560, 2.130, and 2.396 Å, respectively. The results were transformed into the orbitals of $[Mo_3]^{10+}$ at the same Mo–Mo distance.

Basis functions for Mo were obtained from a fitting of Slater-type orbitals (STO's) to Clementi's atomic results.[18] For the 5s and 5p orbitals, exponents of 2.20 were used. The C, O, and Cl functions were a best fit to Herman–Skillman atomic calculations.[19] For hydrogen a single STO with an exponent of 1.16 was used.

Results and Discussion

$[Mo_3]^{12+}$. In order to facilitate a separation of metal–metal and metal–ligand bonding in the triangular systems, it is useful to discuss first the bonding in the "naked" metal triangle $[Mo_3]^{12+}$. In our discussion of this system we find it convenient to employ a coordinate system different from the used in an earlier calculation by one of us.[12b] We use a right-handed local coordinate system on each metal atom in which the z axis points toward the center of the triangle, the x axis is in the plane of the triangle, and the y axis is perpendicular to the plane. Under D_{3h} symmetry, the Mo 4d orbitals in this coordinate system transform as the following irreducible representations:

$$z^2\text{: } a_1' + e'$$

$$x^2 - y^2\text{: } a_1' + e'$$

$$xy\text{: } a_1'' + e''$$

$$xz\text{: } a_2' + e'$$

$$yz\text{: } a_2'' + e''$$

The relative energies and Mulliken percent characters of the principally 4d MO's of $[Mo_3]^{12+}$ are given in Table I. It is

(12) (a) Cotton, F. A.; Haas, T. E. *Inorg. Chem.* **1964**, *3*, 10. (b) Cotton, F. A. *Ibid.* **1964**, *3*, 1217. (c) Cotton, F. A. *Q. Rev., Chem. Soc.* **1966**, *20*, 389.
(13) Cotton, F. A.; Stanley, G. G. *Chem. Phys. Lett.* **1978**, *58*, 540.
(14) Trogler, W. C.; Ellis, D. E.; Berkowitz, J. *J. Am. Chem. Soc.* **1979**, *101*, 5896.
(15) Bursten, B. E.; Cotton, F. A.; Green, J. C.; Seddon, E. A.; Stanley, G. G. *J. Am. Chem. Soc.* **1980**, *102*, 955.
(16) Bursten, B. E.; Cotton, F. A.; Stanley, G. G. *Isr. J. Chem.* **1980**, *19*, 132.
(17) Hall, M. B.; Fenske, R. F. *Inorg. Chem.* **1972**, *11*, 768.
(18) Clementi, E.; Raimondi, D. L. *J. Chem. Phys.* **1963**, *38*, 2686.
(19) Bursten, B. E.; Jensen, J. R.; Fenske, R. F. *J. Chem. Phys.* **1978**, *68*, 3320.

Table II. Relative Orbital Energies, Oxygen Atomic Orbital Contributions, and $[Mo_3]^{12+}$ Contributions for the Occupied Valence Molecular Orbitals of $[Mo_3O_2]^{8+}$

		contribution[a]			
		% oxygen			
orbital	rel E, eV	2s	$2p_\sigma$	$2p_\pi$	$[Mo_3]^{12+}$
$3a_1'$	23.05	0	9		10% $1a_1'$ + 80% $2a_1'$
$2e'$	21.13			9	82% $1e'$ + 9% $2e'$
$2a_2''$	17.84	5	78		17% $1a_2''$
$1e'$	17.63			64	17% $1e'$ + 17% $2e'$
$1e''$	17.18			67	20% $1e''$ + 10% $2e''$
$2a_1'$	16.97	2	53		45% $1a_1'$
$1a_1'$[b]	0.76	91	0		
$1a_2''$	0	86	0		14% $1a_2''$

[a] Dashed entries are zero by symmetry. [b] This level has contributions from high-lying 5s orbitals of $[Mo_3]^{12+}$.

Table III. Relative Orbital Energies, Oxygen Atomic Orbital Contributions, and $[Mo_3]^{12+}$ Contributions for the Occupied a_1' and e' Molecular Orbitals of Mo_3O_6

		contribution[b]		
		% oxygen		
orbital	rel E, eV	2s	2p	$[Mo_3]^{12+}$
$5e'$[a]	23.45		32	22% $1e'$ + 33% $2e'$ + 8% $5e'$
$4a_1'$	19.77		88	10% $3a_1'$
$4e'$	19.55		82	14% $2e'$
$3a_1'$	18.45		41	14% $1a_1'$ + 45% $2a_1'$
$2a_1'$	17.58		14	83% $1a_1'$
$3e'$	17.24		69	5% $1e'$ + 6% $2e'$ + 13% $3e'$
$2e'$	16.63		51	40% $1e'$ + 5% $3e'$
$1a_1'$	0.07	95		
$1e'$	0	94		

[a] Highest occupied orbital. [b] All orbitals contain small contributions from high-lying 5s and 5p orbitals of $[Mo_3]^{12}$.

clear that our choice of local coordinates has resulted in molecular orbitals which retain, to a large extent, the character of only one type of atomic orbital, even when mixing is allowed by symmetry. The $1a_1'$ and $1e'$ orbitals may be regarded as the in-plane, bonding combinations of the Mo $4d_{z^2}$ and $4d_{xz}$ AO's, respectively. The six valence electrons are expected to occupy these orbitals, resulting in a bond order of 1 between each pair of Mo atoms.

This bonding picture of $[Mo_3]^{12+}$ is very similar to that obtained for the metal–metal system of Mo_3O_{13} by use of the CH method.[12b] In that paper the $2a_1'$, $1e''$, $2e'$, and $1a_1''$ orbitals were assumed to be involved primarily in Mo–O bonding and were neglected, resulting in an ordering of bonding orbitals, $a_1 < e < a_1$, and antibonding orbitals, $e < e < a_2$, identical with those reported here. It should be noted that upon lowering the symmetry from D_{3h} to C_{3v} the representations correlate as follows: a_1', $a_2'' \rightarrow a_1$; a_1'', $a_2' \rightarrow a_2$; e', $e'' \rightarrow e$. We shall use these MO's of $[Mo_3]^{12+}$ to assist in the description of the bonding of capping, bridging, and terminal ligands to the metal triangle. We refer to this as the "clusters in molecules" method.

Capping Ligands. The question of how capping ligands bond to the equilateral triangular framework will be addressed first by investigating the electronic structure of the tbp core $[Mo_3O_2]^{8+}$. Neglect of terminally bonded ligands allows us to focus upon the influence of the capping ligands only, without having to sort out those effects due to the terminal ligands; it will be demonstrated later that this is a serviceable approximation. In order to define better how the two capping oxygen atoms perturb the $[Mo_3]^{12+}$ framework, we have transformed the results for $[Mo_3O_2]^{8+}$ into a basis consisting of the oxygen atomic orbitals and the canonical orbitals of the metal triangle.

The relative energies and orbital contributions of the occupied valence levels of $[Mo_3O_2]^{8+}$ are presented in Table II. If the influence of the oxygen atoms does not significantly perturb the metal triangular framework, the oxygen to metal bonding would be expected to occur via donation from the O 2s and $2p_\sigma$ orbitals into empty metal orbitals of a_1' and a_2'' symmetry, and from the O $2p_\pi$ orbitals into empty metal e' and e'' levels. Indeed, it can be seen that the empty $1a_2''$, $1e''$, $2e'$, and $2e''$ orbitals of $[Mo_3]^{12+}$ act as charge acceptors in the $2a_2''$, $1e'$, and $1e''$ MO's of $[Mo_3O_2]^{8+}$. Of greater interest, however, is the behavior of the $1a_1'$ and $1e'$ orbitals of $[Mo_3]^{12+}$, which were fully occupied in the bare triangle. The $2a_1'$ MO of $[Mo_3O_2]^{8+}$ represents a strong bonding interaction between the O 2p AO's and the metal $4d_{z^2}$ orbitals. We believe that this type of interaction is largely responsible for the favorable capping of metal triangles by oxygen atoms. The highest occupied $3a_1'$ MO of $[Mo_3O_2]^{8+}$ is not the antibonding counterpart of the $2a_1'$, for, if it were, the strength of the Mo–O bonding would be diminished. Rather, the strong interaction between the capping oxygen atoms and the $1a_1'$ orbital of $[Mo_3]^{12+}$ favors the transfer of density into the empty $2a_1'$ orbital of $[Mo_3]^{12+}$. If the molybdenum atom contributions to the $3a_1'$ MO of $[Mo_3O_2]^{8+}$ are transformed back into an atomic basis, it is found that this MO closely resembles a symmetric linear combination of $4d_{y^2}$ AO's, i.e., d_{z^2}-like AO's perpendicular to the metal atom plane. The metal–metal bonding resulting from these AO's is not as great as that provided by a "pure" $[Mo_3]^{12+}$ $1a_1'$ orbital, but the cluster has been preserved despite the introduction of metal–oxygen bonding.

The $1e'$ orbital of $[Mo_3]^{12+}$ transfers quite well into the $2e'$ MO of $[Mo_3O_2]^{8+}$, which is lower in energy than the $3a_1'$ orbital. From the orbital characters of the $1e''$, $1e'$, and $2e'$ MO's of $[Mo_3O_2]^{8+}$, it is clear that the π-donating effects of the oxygen atoms are not large enough to force a rehybridization of the metal–metal e' orbitals. Thus, we conclude that the capping oxygen atoms in $[Mo_3O_2]^{8+}$ are bound primarily through Mo–O covalent σ interaction and only in a secondary way by π donation from the oxygen atoms into empty metal–metal orbitals. The $1a_2''$ and $1a_1'$ orbitals of $[Mo_3O_2]^{8+}$ are virtually nonbonding combinations of the filled, low-lying 2s orbitals of the oxygen atoms.

Edge-Bridging Ligands. In order to define the bonding of edge-bridging ligands to the metal triangle in a fashion similar to the preceding discussion of $[Mo_3O_2]^{8+}$, it is desirable to preserve the D_{3h} symmetry of the metal atom triangular system and to exclude from consideration other types of ligands. For these reasons, we have performed molecular orbital calculations on the hypothetical tpr species Mo_3O_6 (**3**), which, thus far, has not been observed in any real compound. The focus of our discussion will be the effect of the bridging ligands upon the occupied metal–metal bonding $1a_1'$ and $1e'$ orbitals of $[Mo_3]^{12+}$. In particular, we are interested in whether the edge-bridging oxygen atoms force a rehybridization of these metal–metal orbitals, as was noted for $[Mo_3O_2]^{8+}$.

The relative energies and percent characters of the occupied valence orbitals of a_1' and e' symmetry in Mo_3O_6 are given in Table III. The $1e'$ and $1a_1'$ MO's of Mo_3O_6 are essentially pure O 2s AO's which do not interact with the metal atoms. The $3e'$, $3a_1'$, $4e'$, and $4a_1'$ MO's of Mo_3O_6 represent donation from the O 2p AO's into empty orbitals of the metal atom triangle; similar ligand to metal donation is seen in orbitals of a_1'', a_2'', and e'' symmetry. The $2a_1'$ MO is the $1a_1'$ metal–metal bonding orbital of $[Mo_3]^{12+}$ perturbed only slightly by the presence of the ligands. Thus the a_1' metal–metal bonding in Mo_3O_6 does not rehybridize as it did in $[Mo_3O_2]^{8+}$. The presence of edge-bridging oxygen atoms does cause the e' metal–metal bonding to rehybridize, however. The

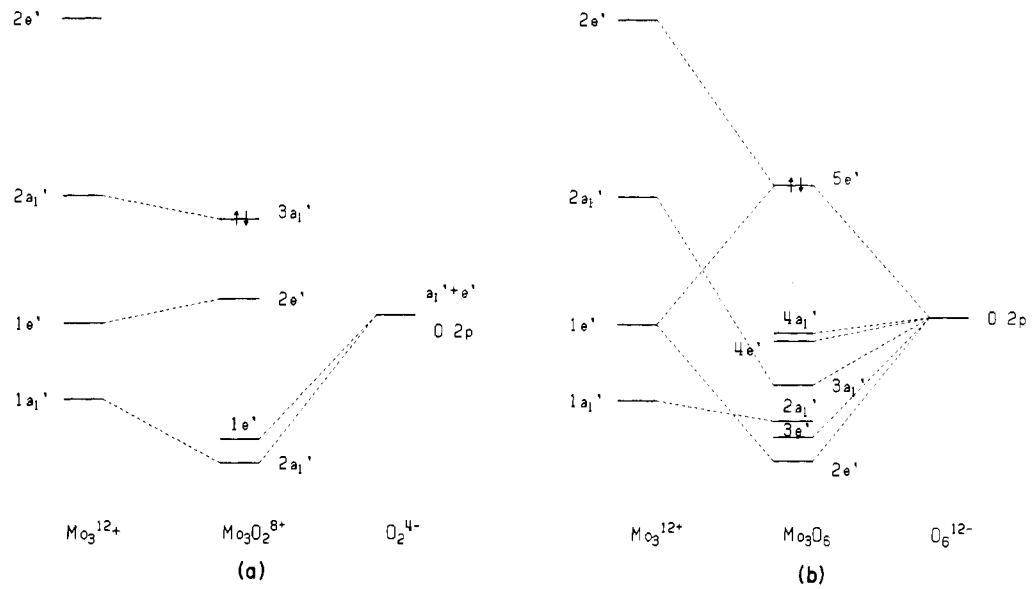

Figure 1. Diagrams showing how the addition of two capping or six edge-bridging ligands affect the energies of the Mo_3^{12+} cluster orbitals.

Table IV. Relative Orbital Energies, Oxygen Atomic Orbital Contributions, and $[Mo_3]^{12+}$ Contributions for the Occupied Valence Molecular Orbitals of $[Mo_3O_4]^{4+}$

		contribution					
		% oxygen[b]					
		capped			bridged		
orbital	rel E, eV	2s	2p	2p	2s	2p	$[Mo_3]^{12+}$ [c]
6e[a]	21.86			5	0	31	34% 1e' + 17% 1e'' + 5% 2e''
$6a_1$	21.68	0	22		0	40	22% $1a_1'$ + 6% $2a_1'$ + 8% $3a_1$
5e	21.14			0	0	71	9% 1e' + 5% 1e'' + 11% 2e'
$5a_1$	19.85	0	0		0	54	42% $2a_1'$
$4a_1$	19.00	0	0		0	35	37% $1a_1'$ + 27% $1a_2''$
4e	18.72			0	0	67	9% 1e' + 8% 3e' + 7% 2e'' + 4% 3e''
$1a_2$	17.93				64	0	34% $1a_2'$
3e	17.83			0	2	56	28% 1e' + 6% 1e'' + 5% 3e'
$3a_1$	17.33	2	58		0	6	27% $1a_1'$ + 7% $1a_2''$
2e	17.30			64	0	0	5% 1e' + 12% 1e'' + 10% 2e' + 5% 2e''
$2a_1$	2.00	4			90	0	5% $3a_1'$
1e	1.64			0	88	0	7% 1e''
$1a_1$	0	88	0		3	0	7% $1a_2''$

[a] Highest occupied molecular orbital. [b] Dashed entries are zero by symmetry. [c] All orbitals contain small contributions from high-lying 5s and 5p orbitals of $[Mo_3]^{12+}$.

2e' MO of Mo_3O_6 indicates strong covalent Mo–O bonding, as was seen in the $2a_1'$ MO of $[Mo_3O_2]^{8+}$. The Mo–O bonding in the 2e' MO is between the Mo $4d_{xz}$ AO's and O 2p orbitals parallel to the plane; similar bonding was seen between the Re and Cl atoms in Re_3Cl_9, in which the edge-bridging ligands lie in the plane of the metal atoms.[15] The strong Mo–O bonding in the 2e' MO of Mo_3O_6 forces a mixing of $[Mo_3]^{12+}$ 2e' character into the predominantly metal 5e' MO of Mo_3O_6. Mo $4d_{x^2-y^2}$ character is mixed with the $4d_{xz}$ orbitals, somewhat weakening the metal–metal bonding in the 5e' MO but preserving the strong metal–oxygen bonding.

The effects of capping and edge-bridging ligands upon the a_1' and e' orbitals which constitute the metal–metal bonding framework are indicated in the interaction diagrams in Figure 1. In each case, some metal–metal bonding is sacrificed to facilitate metal–oxygen bonding. The major difference between the two lies in the source of the Mo–O bonding; the capping ligands interact most strongly with the $1a_1'$ orbital of $[Mo_3]^{12+}$ whereas the edge-bridging ligands are dependent upon the 1e' orbital for their bonding. This dichotomy is consistent with structural differences in metal triangular systems as will be demonstrated later.

$[Mo_3O_4]^{4+}$ and $[Mo_3O_4(OH)_6(H_2O)_3]^{2-}$. The pyr prototype fragment $[Mo_3O_4]^{4+}$ contains both capping and edge-bridging oxygen atoms. As such, it might be expected to exhibit ligand-induced depopulation of both the $1a_1'$ and 1e' MO's of the metal trimer. In this section we will compare the electronic structure of $[Mo_3O_4]^{4+}$ with those of the tbp and tpr species in order to determine the dominant bonding modes when both types of ligand are present. In addition we will discuss the electronic structure of the pyr species $[Mo_2O_4(OH)_6(H_2O)_3]^{2-}$ in order to see how the terminal ligand to metal atom bonding arises and to see if our use of core fragments in the investigation of metal–oxygen bonding modes is a satisfactory approximation. The relative energies and percent characters of the occupied valence orbitals in $[Mo_3O_4]^{4+}$ are listed in Table IV.

The valence electronic structure of $[Mo_3O_4]^{4+}$ is compared to those of $[Mo_3O_2]^{8+}$ and Mo_3O_6 in the molecular orbital diagram of Figure 2. The MO diagram indicates that the electronic structure of the pyr species is indeed intermediate between those of the tbp and tpr types. In Table V the Mulliken populations of the canonical orbitals of $[Mo_3]^{12+}$ in the tbp, pyr, and tpr species are compared. For $[Mo_3O_2]^{8+}$ it is seen that 0.81 e is promoted out of the $1a_1'$ MO while the 1e' is scarcely depopulated. This situation is reversed for Mo_3O_6, in which 1.06 e is removed from the 1e' orbital with essentially no density removed from the $1a_1'$. The populations

Table V. Mulliken Populations of the Canonical Valence Orbitals of $[Mo_3]^{12+}$ for $[Mo_3(\mu_3\text{-}O)_2]^{8+}$, $[Mo_3(\mu\text{-}O)_6]$, $[Mo_3(\mu_3\text{-}O)(\mu\text{-}O)_3]^{4+}$, $[Mo_3(\mu_3\text{-}O)(\mu\text{-}O)_3(OH)_6(H_2O)_3]^{2-}$, and $[Mo_3(\mu_3\text{-}O)_2(O_2CH)_6(H_2O)_3]^{2+}$ and of the Canonical Valence Orbitals of $[Mo_3]^{10+}$ for $[Mo_3(\mu_3\text{-}O)(\mu\text{-}Cl)_3]^{5+}$

	six-electron systems						eight-electron systems	
orbital	$[Mo_3]^{12+}$	$[Mo_3O_2]^{8+}$	$[Mo_3O_6]$	$[Mo_3O_4]^{4+}$	$[Mo_3O_{13}H_{12}]^{2-}$	$[Mo_3O_{17}C_6H_{12}]^{2+}$	$[Mo_3]^{10+}$	$[Mo_3OCl_3]^{5+}$
$1a_1'$	2.00	1.19	1.96	1.78	1.77	0.79	2.00	1.90
$1e'$	4.00	3.94	2.94	3.45	3.45	3.80	4.00	3.74
$1a_2''$		0.64	0.88	0.84	0.88	0.52	2.00	0.86
$2a_1'$		1.64	0.99	0.98	1.69	1.92		1.89
$1e''$		0.80	1.28	1.85	1.79	1.44		1.91
$2e'$		1.03	2.18	1.05	1.05	1.15		1.25
$1a_1''$		0.00	0.80	0.65	0.62	0.62		0.86
$3e'$		0.00	0.93	0.70	0.83	1.21		0.69
$2e''$		0.39	0.67	0.71	0.96	0.95		0.50
$1a_2'$		0.00	0.00	0.00	0.13	0.25		0.04

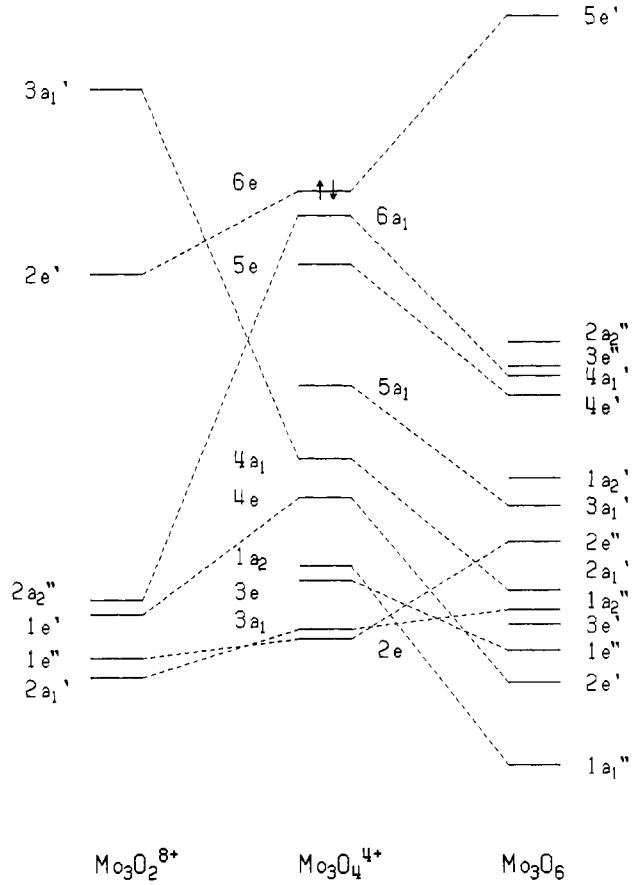

Figure 2. Comparison of MO types and energies for the three capped and/or bridged Mo_3 cluster species.

for $[Mo_3O_4]^{4+}$ indicate that the influence of the edge-bridging ligands is greater than that of the capping ligand: 0.22 e is removed from the $1a_1'$ orbital while 0.55 e is transferred out of the $1e'$ orbital.

The high Mulliken population of the canonical $1e''$ orbital in $[Mo_3O_4]^{4+}$ is quite interesting. The reason for this high population, greater than that in either $[Mo_3O_2]^{8+}$ or Mo_3O_6, is the lower symmetry of the pyr species. When the symmetry is lowered from D_{3h} to C_{3v}, the e' and e'' representations both correlate to e symmetry, i.e., the symmetry or antisymmetry about the horizontal mirror plane is lost. In $[Mo_3O_4]^{4+}$ this symmetry lowering results in strong mixing between the $1e'$ and $1e''$ orbitals, that is, between the Mo $4d_{xz}$ and $4d_{xy}$ AO's. The resulting hybrid orbitals are tipped out of the plane of the metal atoms toward the capping oxygen atom, facilitating better overlap with both the capping and, especially, the edge-bridging oxygen atoms. We believe that it is this rehybridization, allowed under C_{3v} symmetry, which makes possible better metal–ligand bonding with only a small sacrifice of metal–metal bonding, that largely accounts for the proliferation of pyr species of the general formulation M_3X_{13}.

Until this point in the discussion we have tacitly assumed that the $[Mo_3O_2]^{8+}$ and $[Mo_3O_4]^{4+}$ "cores" can be used as reasonable models for the bonding in Mo(IV) tbp and pyr species in which peripheral ligands are also present to complete the Mo coordination spheres. To test the validity of this assumption, we have performed a calculation on the pyr species $[Mo_3O_4(OH)_6(H_2O)_3]^{2-}$, a model for the structurally characterized compound $[Mo_3O_4(C_2O_4)_3(H_2O)_3]^{2-}$, in which each bridging oxalato ligand has been approximated by two hydroxyl groups. The resulting $[Mo_3]^{12+}$ canonical orbital populations are given in Table V. It is seen that the major effect of including the peripheral ligands is an increase in the populations of the $2a_1'$ and, to a much lesser extent, the $3e'$ and $2e''$ orbitals. This represents terminal ligand donation primarily to the Mo $4d_{x^2-y^2}$ orbitals with lesser donation to the $4d_{yz}$ AO's. Most important to the present discussion is the negligible effect of the terminal ligands upon the populations of the canonical $1a_1'$ and $1e'$ orbitals; these are virtually identical with the populations obtained from the calculation on $[Mo_3O_4]^{4+}$. It is clear then that the core fragment analysis is a good approximation for determining the effects of capping and bridging ligands upon the electronic structure of the metal atom triangle.

Variable Electron Population in Pyr Species. Recently, the structural characterization of the pyr species $[Mo_3OCl_3(O_2CCH_3)_3(H_2O)_3](ClO_4)Cl$, a product of the reaction of $Mo(CO)_4Cl_2$ with acetic acid/acetic anhydride, was reported.[7] The molybdenum atoms in this species achieve a crystallographically imposed equilateral triangular configuration with a Mo–Mo bond distance of 2.550 (2) Å. A reckoning of the metal valence electrons gives a total of eight, two more than are found in pyr species containing the $[Mo_3O_4]^{4+}$ moiety. To determine how the additional electrons occupy the triangular system, we have performed a Fenske–Hall calculation on the eight-metal-electron pyr core $[Mo_3OCl_3]^{5+}$.

The eight valence electrons of the metal atom triangle $[Mo_3]^{10+}$ fully occupy the $1a_1'$, $1e'$, and $1a_2''$ orbitals. The latter orbital has been assumed to be primarily involved in metal–ligand bonding,[12] however, and the two additional electrons in $[Mo_3OCl_3]^{5+}$ have been predicted to occupy the $2a_1'$ orbital. The Mulliken populations for $[Mo_3OCl_3]^{5+}$, given in Table V, would seem to justify this analysis. The $1a_2''$ canonical orbital has virtually the same population as in $[Mo_3O_4]^{4+}$ or $[Mo_3O_4(OH)_6(H_2O)_3]^{2-}$, indicating that it is accepting ligand charge to about the same extent. The $1a_1'$ and $1e'$ orbitals have slightly higher populations than in $[Mo_3O_4]^{4+}$, most probably the result of a greater energetic separation (and hence less interaction) of the ligand p orbitals and the Mo 4d AO's because of the reduction in Mo oxidation state from +4 to $+3\ ^1/_3$. Most of the additional metal electron

density indeed goes into the $2a_1'$, which has 0.9 e greater population in $[Mo_3OCl_3]^{5+}$ than in $[Mo_3O_4]^{4+}$.

In light of these results it is pertinent to consider the reasons for the greater Mo–Mo bond length in $[Mo_3OCl_3(O_2CCH_3)_3(H_2O)_3]^{2+}$ than in $[Mo_3O_4(C_2O_4)_3(H_2O)_3]^{2-}$ (2.550 vs. 2.486 Å). The greater total population in the bonding $1a_1'$ + $1e'$ orbitals in $[Mo_3OCl_3]^{5+}$ than in $[Mo_3O_4]^{4+}$ would seem to favor shorter Mo–Mo bonds in the former rather than the latter species. Three effects counter this argument, however: (1) the replacement of μ-O atoms by larger μ-Cl atoms favors a lengthening of the Mo–Mo bonds in order to avoid a reduction of the Mo–(μ-ligand)–Mo angle; (2) the reduction of the effective metal charge from +4 to $+3^1/_3$ should be accompanied by an increase in the effective atomic radius of the Mo atoms for the eight electron system; (3) the increased occupation of the $2a_1'$ orbital will accommodate a greater occupation of metal–metal antibonding orbitals. This last effect requires some explanation. The $2a_1'$ orbital is essentially the symmetric linear combination of Mo $4d_{x^2-y^2}$ AO's. As such, it is weakly bonding and its increased occupation would not be expected to lengthen the Mo–Mo bonds. It was shown previously, however, that the major mode of peripheral ligand bonding in $[Mo_3O_4(OH)_6(H_2O)_3]^{2-}$ was via donation into the $2a_1'$ orbital. This orbital will be unavailable for charge acceptance in the eight-electron system and, most likely, the peripheral ligands will donate primarily into the weakly antibonding $2e'$ orbital. It is not apparent which of these three effects plays the dominant role in lengthening the Mo–Mo bond in the eight-electron pyr system; clearly the structural characterization of compounds containing elusive $[Mo_3O_4]^{2+}$ or $[Mo_3OCl_3]^{7+}$ pyr cores would aid in evaluating the relative importance of metal charge and ligand-type effects.

Tbp vs. Pyr Six-Electron Systems: Structural Implications. The selective ligand-induced depopulation of the metal–metal bonding $1a_1'$ and $1e'$ MO's by capping and edge-bridging ligands should profoundly affect the extent of bonding in the metal triangle. In light of the rapidly growing body of structural comparisons between tbp and pyr compounds, it is pertinent to discuss the implications of our calculations on the metal–metal bonding in these systems.

As discussed previously, the six valence electrons of a triangle of Mo(IV) atoms will fully occupy the $1a_1'$ and $1e'$ orbitals, resulting in single bonds between each pair of molybdenum atoms. The $1a_1'$ MO, the symmetric linear combination of Mo $4d_{z^2}$ AO's, represents a stronger contribution to the metal–metal bonds than does either component of the $1e'$ orbital; this comparison has been discussed in detail in connection with the bonding in Re_3Cl_9.[14] Depopulation of either the $1a_1'$ or $1e'$ orbital will result in a weakening of the metal–metal bonding, but it should be more pronounced for the former.

The presence of capping (μ_3) or bridging (μ) ligands disrupts the bonding in the $1a_1'$ and $1e'$ orbitals, respectively. Inspection of the results for Mo_3O_6 and $[Mo_3O_2]^{8+}$ in the Table V indicates that the effect of six bridging ligands is roughly equivalent, in a depopulating sense, to two capping ligands. Extending this to a comparison of $[Mo_3O_4]^{4+}$ and $[Mo_3O_2]^{8+}$, we find that the $1a_1'$ + $1e'$ populations in each of these species is nearly the same: 5.33 e in the pyr one and 5.13 e in the tbp. The population of $1a_1'$ MO is much greater in $[Mo_3O_4]^{4+}$, however, and it is to be expected that the Mo–Mo bonds in pyr compounds are shorter than those of tbp geometry.

The above analysis has neglected the effect of higher lying metal–metal levels, however. As an example it could be argued that the density residing to the antibonding $3e'$ MO for $[Mo_3O_4]^{4+}$ would offset the bonding due to the $1a_1'$ orbital. A proper comparison of pyr and tbp structures must involve a consideration of the geometric and electronic effects of the peripheral ligands. For this reason we have performed a calculation on $[Mo_3(\mu_3\text{-}O)_2(O_2CH)_6(H_2O)_3]^{2+}$, a molecule with a tbp core, two carboxylato ligands bridging each Mo–Mo bond, and a terminally bound water molecule on each Mo atom. This structural unit has been characterized with tungsten atoms as well.[4] The results are summarized in Table V. For the tbp species, the greater number of carboxylato ligands and the presence of water molecules in the metal atom plane result in much greater donation from the peripheral ligands into antibonding metal–metal orbitals than is found for the pyr geomtry. The net result is approximately the same populations of the high-lying $2e'$–$1a_2'$ canonical $[Mo_3]^{12+}$ orbitals in each species. Thus, the metal–metal bond in the pyr compounds should indeed be shorter than those in the tbp compounds.

The structural data available on the pyr and the tbp compounds confirm that the Mo–Mo bonds are significantly shorter in pyr compounds than they are in tbp ones: 2.49 Å in $[Mo_3O_4(C_2O_4)_3(H_2O)_3]^{2-}$ vs. 2.75 Å in $[Mo_3O_2(O_2CCH_3)_6(H_2O)_3]^{2+}$. This lengthening by 0.26 Å is most certainly due in part to the difference in the distribution of charge density in the molecules.

Finally, it is amusing to conjecture on the existence of six-electron tpr species. Electronically, these compounds would be expected to have greater density in the $1a_1'$ orbital than either the pyr or tbp species, and as such might be expected to have Mo–Mo even shorter than 2.49 Å. The problem with the tpr geometry, however, may be the accommodation of terminal ligands. It seems doubtful that carboxylato groups would be favorably disposed to bridging two molybdenum atoms in the plane of the ring; such a gometry would lead to unfavorable steric interaction between the carboxylato and the μ-O groups. It may be possible to stabilize such a species if only monodentate terminal ligands are used, however, avoiding interactions between the terminal and edge-bridging ligands.

Acknowledgment. We thank the National Science Foundation for support.

Registry No. Mo, 7439-98-7; W, 7440-33-7.